J. Chem. Phys. 48, 3779 (1968).

[19]D. Stukel, R. Euwema, T. Collins, F. Herman, and R. Kortum, Phys. Rev. 179, 740 (1969).

[20]U. Rössler, Phys. Rev. 184, 733 (1969).

[21]M. Cohen and T. Bergstresser, Phys. Rev. 141, 789 (1966).

[22]F. Herman, R. Kortum, C. Kuglin, and J. Shay, in

Proceedings of the International Conference of II-VI Semiconducting Compounds, Providence, 1967, edited by D. Thomas (Benjamin, New York, 1967), p. 503.

[23]H. Overhof (private communication).

[24]R. Hengehold, R. Almassy, and F. Pedrotti, Phys. Rev. B 1, 4784 (1970).

Electron-Irradiation Effects in Silicon at Liquid-Helium Temperatures Using ac Hopping Conductivity*

R. E. McKeighen and J. S. Koehler

Nuclear Engineering Program, Department of Physics, and Materials Research Laboratory, University of Illinois, Urbana, Illinois 61801

(Received 25 February 1971)

Changes in ac hopping conductivity with electron irradiation have been measured in n-type, p-type, and high-purity silicon. Irradiations were carried out at both 5.0 and 1.6 °K, with measurements made at reference temperatures of 4.2 and 1.3 °K, respectively. In the p-type crystals, the changes in ac hopping conductivity depend strongly on the concentration of chemical acceptors, indicating a concentration dependence on impurities in the defect production rate. The production rates at 1.6 °K were generally very similar to those for a 5.0 °K irradiation. No significant thermal annealing stages below room temperature were observed in any of the crystals. No radiation annealing effects due to a beam of either 0.500-MeV or 0.350-MeV electrons were observed, either at 4.5 or 1.45 °K. The possibility of athermal effects leading to interstitial migration is suggested.

I. INTRODUCTION

Radiation effects in semiconductors, particularly silicon and germanium, have been studied since the early 1950's. Early research had two motivating emphases: (i) determining defect yields resulting from exposure to a variety of radiations in order to check the simple theory of defect displacements; (ii) constructing defect models to account for the multitude of energy levels produced in terms of simple Frenkel defects. Although this field has not suffered from lack of experimental data, some of the most fundamental questions are still being asked. (a) What are the impurities? (b) What moves at the lowest irradiation temperature, and what is that temperature? (c) Where is the interstitial? (d) What is the configuration of the interstitial?

Watkins's[1] EPR measurements indicated that the vacancy in p-type silicon is mobile in the temperature range around 160 °K and that the vacancy in n-type silicon is mobile in the range 60–80 °K.

The self-interstitial in silicon has never been observed. It is believed to be mobile even during a liquid-helium-temperature irradiation because of the following observation made by Watkins. Isolated vacancies and interstitial aluminum atoms (Al++) were produced in approximately 1:1 correspondence (~ 0.03 defects/cm³ per electron/cm²) by 1.50-MeV

electron irradiation. Now, for every vacancy formed in a primary radiation damage event, there must also be an interstitial atom. Watkins suggested that the interstitial silicon atom migrates through the lattice until trapped by the substitutional aluminum atom. In the trapped state, the silicon atom replaces the substitutional aluminum atom, ejecting it into the interstitial site. The end result is a vacancy and an interstitial aluminum atom well separated from each other.

The motivation for the present experiment was to see if the interstitial is indeed mobile during a liquid-helium-temperature irradiation using some observation different from EPR. The difficulty in silicon is that normal electrical measurements depend on free carriers in the crystal; they are frozen out at temperatures below about 30–40 °K so that dc electrical conductivity becomes very small. Measurement of ac hopping conductivity, however, can be made down to below 1 °K. The present measurements show that ac hopping conductivity can be used as a tool for studying radiation effects in silicon.

II. DISCUSSION OF ac HOPPING CONDUCTIVITY

If one considers a crystal doped with only one kind of impurity, say, n-type impurities of concentration N_d, at $T = 0$ °K, all of the electrons that are thermally excited from the donors into the conduc-

tion band at higher temperatures will be frozen into the donor levels; thus all of the donors are occupied and neutral. On the other hand if the crystal is partially compensated, containing a concentration of acceptors N_a, where N_a is less than N_d, then at $T = 0\,°K$ a number of the donors equal to N_a will have given up their electrons to the lower-lying acceptor levels. The net result is that there will be N_a negatively charged acceptors in the crystal and N_a positively charged, or unoccupied, donor levels. There will also be $N_d - N_a$ occupied donor levels. The compensation ratio K is the ratio of minority to majority impurity concentration, i.e., $K = N_a/N_d$. Because of the Coulombic forces between the ionized impurities, the state of lowest energy is achieved when the majority impurity nearest a given minority impurity is ionized.[2] On application of a steady electric field, a current can be perpetuated only if thermal energy is sufficient to overcome the Coulombic potential around the minority impurity. The only charge transitions which can yield a net transport of charge at low impurity concentration and low temperatures are those from occupied (neutral) to vacant (unoccupied) majority impurities. The model is that of phonon-assisted tunneling of an electron (or hole) from an occupied donor (acceptor) site to an unoccupied site in the presence of the Coulomb fields arising from compensating acceptors and ionized donors. On the other hand, even if there is insufficient thermal energy, the potential can be altered by an applied ac electric field and a new equilibrium has to be established. This will take a time of the order of the hopping time or tunneling time and a net polarization will occur. The rate of polarization can be detected as a current in an ac experiment.

At sufficiently high frequencies, contributions to the conductivity from multiple hops can be neglected and only hops between pairs of impurities have to be considered. In general, the part of the polarization which is out of phase with the field is measured as a dielectric loss or ac conductivity. Similarly,

the in-phase part of the polarization makes a contribution to the dielectric constant.[3] These real and imaginary parts of the conductivity of the samples can best be determined from capacitance C and dissipation factor D measurements on a capacitance bridge.

One expects the ac hopping conductivity to reach a maximum value at a compensation ratio of about $K = 0.5$. This is because for low K there are only a few empty sites to which the electrons can jump, while at high K there are only a few electrons available to make the jumps.

We shall start with an uncompensated crystal doped primarily with either an n- or p-type impurity. The defects introduced by electron irradiation at $5\,°K$ would then serve as the compensating minority impurity and give rise to the ac hopping conductivity.

Pollak and Geballe,[2] making measurements on silicon samples containing known majority and minority impurity concentrations, found experimentally that σ_{ac}, the ac conductivity, is given by

$$\sigma_{ac} = k\omega^{0.8} N_{min}{}^{0.85},$$

where k is a constant for a fixed temperature, ω is the frequency of the ac signal, and N_{min} is the concentration of compensating minority impurities. They found that σ_{ac} is essentially independent of the majority impurity concentration.

As will be discussed in Sec. V (Fig. 23), in p-type silicon, one expects the interstitial to be positively charged and the vacancy to be neutral when the Fermi level is pinned to the acceptor level at these low temperatures. Therefore, the interstitials (silicon or a group-III impurity) will act as compensating minority impurities in a p-type lattice and one expects σ_{ac} to be proportional to their concentration.

Similarly in n-type silicon one expects the interstitial to be neutral (or positive), whereas the vacancy probably has a double negative charge. In this case the vacancies act as the minority impurity

TABLE I. Crystals irradiated and studied using ac hopping conductivity.

Type	Dopant	Supplier	Growth method	Resistivity (Ω cm)	Dopant concentration
p	Aluminum	TI[a]	Lopex (FZ)	4.0	3.3×10^{15}
p	Aluminum	TI	Pulled	0.37	5.0×10^{16}
p	Aluminum	TI	Pulled	0.10	5.0×10^{17}
p	Boron	Semi-element	(FZ)[b]	0.60	3.0×10^{16}
p	Boron	Monsanto	(FZ)	0.27	1.0×10^{17}
n	Phosphorus	Monsanto	Monex (FZ)	5.34	1.0×10^{15}
n	Phosphorus	Monsanto	Monex (FZ)	0.54	1.1×10^{16}
n	Phosphorus	Semi-elements	Pulled	0.08	1.3×10^{17}
High purity	Boron	TI	(FZ)	500–1000	$\sim 10^{13}$

[a]TI, Texas instruments.   [b]FZ, Float zone.

and one expects σ_{ac} to be proportional to their con-
centration, but independent of the interstitial con-
centration.

III. EXPERIMENTAL DESCRIPTION

A. Sample Preparation

Samples studied in this experiment were cut from
single-crystal ingots obtained from either Texas
Instruments, Monsanto, or Semi-Elements and were
either float zone refined or grown by the Czochral-
zki technique (pulled). The single-crystal ingots
were typically 1 in. in diam and approximately 6 in.
long. The various crystals used in this study are
summarized in Table I. The crystals had disloca-
tion densities less than $500/cm^2$.

For an ac measurement, it is not necessary that
the contacts be nonrectifying or Ohmic. Pollak and
Geballe[2] found that simple gold contacts electro-
plated on lapped surfaces gave the same results as
heavily doped N^+ contacts prepared by diffusing
phosphorus into the surface of n-type silicon. The
final lapped specimens were $0.015 \times 1.5 \times 1.5$ cm.
Gold electrodes $\frac{1}{4}$ in. diam were evaporated onto the
two large faces.

The silicon devices were mounted on a $\frac{1}{16}$-in.-
thick quartz plate by attaching one edge of the slice
with GE No. 7031 varnish. This quartz plate had
outer dimensions of $1\frac{1}{2} \times 1\frac{7}{8}$ in. and had a rectangular
hole in the middle $1 \times \frac{3}{4}$ in. through which the
electron beam passed. Four silicon devices were
mounted around this hole in such a manner that the
$\frac{1}{4}$-in.-diam gold electrodes on the silicon surface
were placed inside the area of this hole. Electrical
leads were attached to the gold electrodes using
silver micropaint.

The quartz plate with the four samples mounted
and leads attached was placed on top of a gold-
plated $\frac{1}{16}$-in.-thick copper plate of identical dimen-
sions as the quartz plate. The pair of plates was
then mounted in the sample chamber of the liquid-
helium cryostat, attached to the two pillars by four
No. 1-72 screws (Fig. 2). The loose ends of the
wire leads were then attached to the pin block in
the sample chamber which had wires leading up
the Dewar to external connectors.

B. Cryostat and Sample Chamber

The liquid-helium cryostat used in this experi-
ment is a 5-liter Dewar purchased from Superior
Air Products Co., Newark, N.J. A schematic
drawing of the cryostat arrangement as used in this
experiment is shown in Fig. 1. A rigid tail section
was built and attached to the bottom of the com-
mercial Dewar to give the liquid-helium tail rigid-
ity. The sample chamber was attached to the bot-
tom of the rigid tail section. The details of the
sample chamber are shown in Fig. 2.
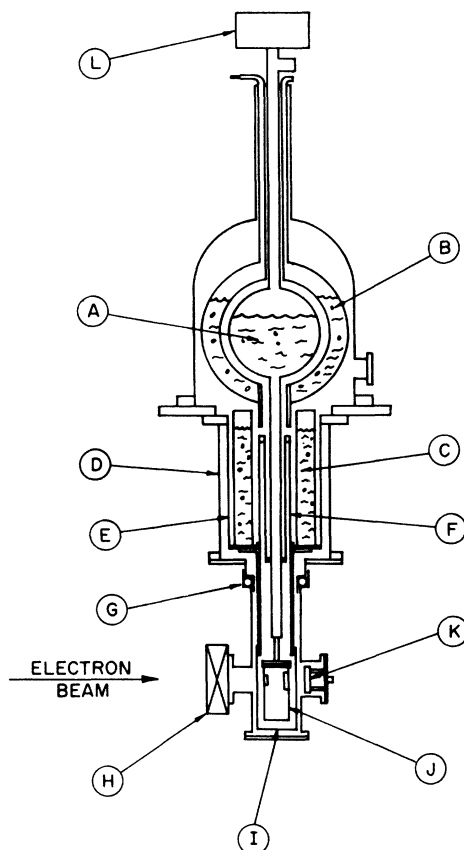
FIG. 1. Schematic of liquid-helium cryostat for
electron irradiation studies: (a) 5-liter liquid-helium
reservoir; (b) 12-liter capacity liquid-nitrogen reser-
voir; (c) 7-liter liquid-nitrogen reservoir surrounding
tail section of liquid-helium reservoir; (d) rigid tail
section; (e) 0.010-in. stainless-steel cylinder support-
ing liquid-nitrogen reservoir; (f) 0.006-in. stainless-
steel concentric cylinders giving liquid-helium tail
rigidity; (g) ball-bearing race for rotating Dewar and
sample chamber relative to beam; (h) 2-in. gate valve
for hook up to Van de Graaff; (i) copper cylinder at
liquid-nitrogen temperature with 0.007-in. aluminum-
coated Mylar windows for electron beam; (j) sample
chamber holding exchange gas around samples and
having entrance and exit windows for the electron beam
of 0.002-in. Duraluminum; (k) beam stop and beam
current monitor mounted on room-temperature cylinder;
(l) vacuum-tight enclosure for introduction of exchange
gas to the sample chamber and for wire leads running
down to the sample.

C. Temperature Measurement

The temperature of the samples was monitored
by measuring the resistance of a carbon resistor
mounted next to the samples on the quartz plate.
The resistors were Allen-Bradley, type AB, $\frac{1}{8}$ W,
with a nominal room-temperature resistance of
200 Ω and a liquid-helium-temperature resistance
of about 3000 Ω. These thermometers were cali-
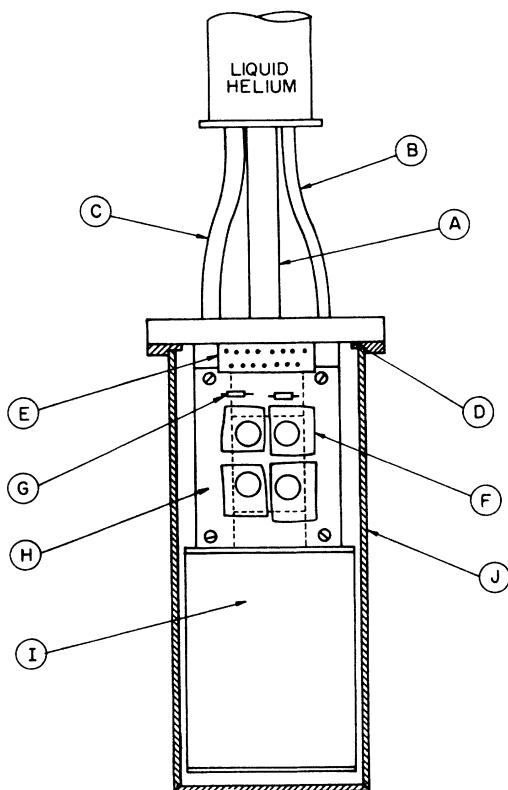
FIG. 2. View of sample mounting chamber: (a) $\frac{5}{16}$-in.-diam × 0.006-in.-thick inconel tube carrying exchange gas and lead wires to sample chamber; (b) $\frac{1}{8}$ in.-diam-×0.004-in.-thick inconel tube carrying liquid helium to the reservoir in sample chamber, with a needle-valve flow control positioned above this tube; (c) $\frac{3}{16}$-in.-diam.×0.006-in.-thick inconel tube for venting helium gas; (d) demountable indium o-ring seal for removing outer cylinder to mount samples; (e) strip of Teflon with copper pins to which wires are attached leading up to top of Dewar and to which wire leads on samples can be readily attached; (f) $\frac{1}{16}$-in. quartz plate with four silicon samples mounted; (g) carbon resistor thermometer; (h) copper posts $\frac{3}{8}×\frac{9}{16}$ in. to which quartz plate is mounted and which are hollowed out so that the reservoir can be filled with liquid helium and vented (note that these hollow posts are also filled with liquid helium during irradiation); (i) $1\frac{3}{4}$-in.-diam hollow copper cylinder holding a reservoir of 68 cm^3 of liquid helium; the heater wire is wrapped around this cylinder; (j) copper cylinder holding helium exchange gas around samples and having entrance and exit windows for the electron beam of 0.002-in. Duraluminum.

brated in resistance vs temperature using a calibration equation having the resistance at liquid-helium and liquid-nitrogen temperatures as the two calibration points.

For temperatures below 4.2 °K, the equilibrium pressure above the liquid helium was reduced by a Welch Duo-Seal rotary vacuum pump, model 1398,

which has a pumping speed of 23 liters/sec. The lowest temperature which could be reached with this arrangement was 1.3 °K. To efficiently lower the temperature in this manner, the pumping speed of the pump was initially throttled down by a needle valve in conjunction with a Veeco vacuum valve.

Below 4.2 °K, the carbon resistor was calibrated against the vapor pressure above the liquid-helium bath, measured with a Wallace-Tiernan pressure gauge having a range 1–50 mm Hg. This calibration was made as the liquid helium was being pumped down. As the temperature is dropping due to the pumping operation, there is turbulance and bubbles formed which help to keep the liquid helium at a uniform temperature from top to bottom, assuring one that the temperature at the surface of the liquid and at the carbon resistor at the bottom of the Dewar are the same. Furthermore, below the λ point liquid helium has a high thermal conductivity, eliminating any temperature gradients that would effect the calibration of the carbon resistors against the vapor pressure. The calibration curve derived by extending the calibration equation below 4.2 °K agreed well with that obtained from the vapor pressure of the bath.

The objection could be raised that the temperature measured by the carbon resistor is that of the quartz plate and not of the silicon slice in the beam. However, a calculation shows that this temperature difference is less than 0.1 °K. In an experimental check at 5 °K with one carbon resistor mounted directly on the silicon in the beam and one mounted on the quartz plate next to the silicon, the temperature difference between these two carbon resistors was always less than 0.1 °K.

In addition to the cooling provided by the thermal conductivity of the silicon itself, additional cooling is provided by the helium exchange gas surrounding the sample and providing an additional thermal path to the liquid-helium reservoir. The exchange gas cools by both thermal conduction and convection currents. An exchange gas pressure of 1 atm was introduced while the Dewar was at room temperature, so that at liquid-helium temperature, the exchange-gas pressure is around 10 mm Hg.

D. Data Acquistion and Analysis

The ac hopping conductivity was determined by measuring the capacitance and the dielectric loss (or dissipation factor D) of the samples using a General Radio model 1615-A capacitance bridge with a PAR model HR8 lock-in amplifier used as both the signal generator and the null detector for the bridge. Transformer ratio arms are used in this bridge giving it a capability of six-figure resolution in capacitance and four-figure resolution in dissipation factor. Using this bridge, values of ac conductivity could be measured ranging from 6

$\times 10^{-15}$ $(\Omega\,\text{cm})^{-1}$ to 3×10^{-9} $(\Omega\,\text{cm})^{-1}$ at a frequency of 1 kHz. The bridge allows a three-terminal measurement so that any capacitance of the leads to ground are excluded, thus allowing long coaxial leads to be used without affecting the measured value of the capacitance of the samples. The capacitance between the leads without any samples connected was about 0.001 00 pF. Measurements were made at frequencies from 0.1 to 100.0 kHz.

The direct measurements of the capacitance and the loss factor D are directly related to the real and imaginary parts of the ac hopping conductivity. The real part is obtained from the formula

$$\sigma_{\text{ac}} = \text{Re}(\sigma) = [D\omega C_s/(1+D^2)](d/a) ,$$

where d/a is the geometric factor, with d the thickness of the slice and a the area of the electrode. $\omega = 2\pi f$, where f is the frequency in cycles per second. The imaginary part of the ac conductivity is given by

$$\text{Im}(\sigma) = \omega C_{\text{pol}} ,$$

where $C_{\text{pol}} = C_s - C_0$ and C_0 is the capacitance due to the dielectric constant of silicon plus the capacitance between leads. For samples with $\frac{1}{4}$-in.-diam electrodes about 125 μ thick, C_s typically had a value of 40–50 pF. Since C_0 makes up the biggest part of the capacitance, C_{pol} and consequently $\text{Im}(\sigma)$ are difficult to determine with accuracy. However, $\text{Re}(\sigma) = \sigma_{\text{ac}}$ is easily determined. In most of the samples studied, $D \ll 1$, so that the D^2 term in the expression for σ_{ac} could be ignored. Furthermore, since C_0 typically accounts for 99% of the measured capacitance and since the capacitance typically did not change much with irradiation, except for the highly boron-doped sample, we may approximate

$$C_s \cong C_0 = k\epsilon_0(a/d) ,$$

where k is the dielectric constant of silicon. We used the value $k = 11.5$. Making these substitutions into the expression for σ_{ac}, we have the simpler form, valid for most of the samples studied,

$$\sigma_{\text{ac}} = D\omega k\epsilon_0 = 6.395 \times 10^{-9} f' D,$$

where f' is the frequency in kilohertz.

E. Irradiation and Annealing Procedure

The irradiations were performed using the Materials Research Laboratory Van de Graaff electron accelerator. The energy of the electrons was set at 1.0, 1.5, or 2.0 MeV. Beam currents ranged from 1.2 to 2.0 $\times$ 10^{-8} A/cm^2. The electron beam was allowed to pass completely through the sample chamber and was stopped in a $\frac{3}{16}$-in.-thick brass plate at room temperature. The current to this plate was measured and integrated on an Elcor current integrator model (A309B) to give the total

electron fluence.

Thermal anneal experiments were performed after moving back into the laboratory, although they could have also been done while still in the accelerator room. To do an anneal, the needle valve was first closed off, cutting off the supply of liquid helium to the sample chamber. The exchange pressure was also usually reduced to about 30 μ. A current of about 170 mA was put through the 500-Ω heater for a few minutes to bring the samples up to the desired temperature. A temperature control circuit making use of a Simpson milliampere relay meter gave small current changes in addition to a constant base heater current to help maintain a given temperature more readily. The samples were held at a given temperature for 10 min for isochronal anneals, at which time the current was shut off and the needle valve was reopened, allowing the sample chamber to refill with liquid helium and returning the sample temperature quickly to 4.2 °K.

IV. EXPERIMENTAL RESULTS

To decide whether the changes observed are to be associated with changes in surface conductivity or with bulk changes, four samples with electrodes placed a centimeter apart on the bombarded surface were measured. Two intrinsic, one n- and one p-type, specimens were used. With various energies from 0.300 to 2.0 MeV and a total fluence up to 1.4×10^{16} e^-/cm^2, changes in the surface conductivity were too small to measure. This puts an
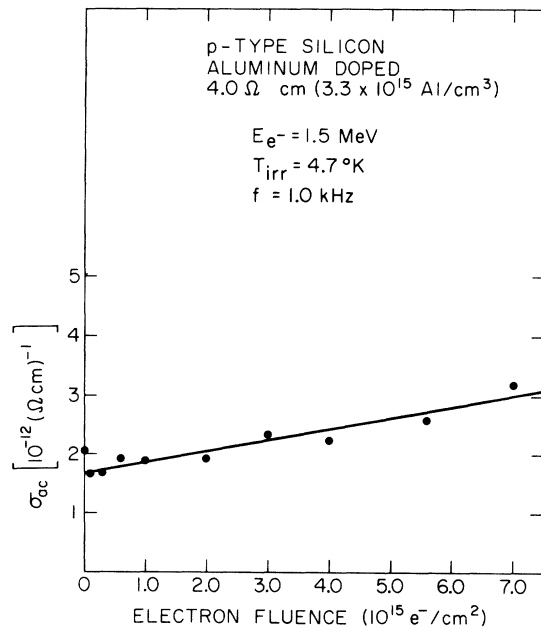
FIG. 3. Changes in σ_{ac} with irradiation for 4.0-Ω-cm p-type silicon, aluminum doped.
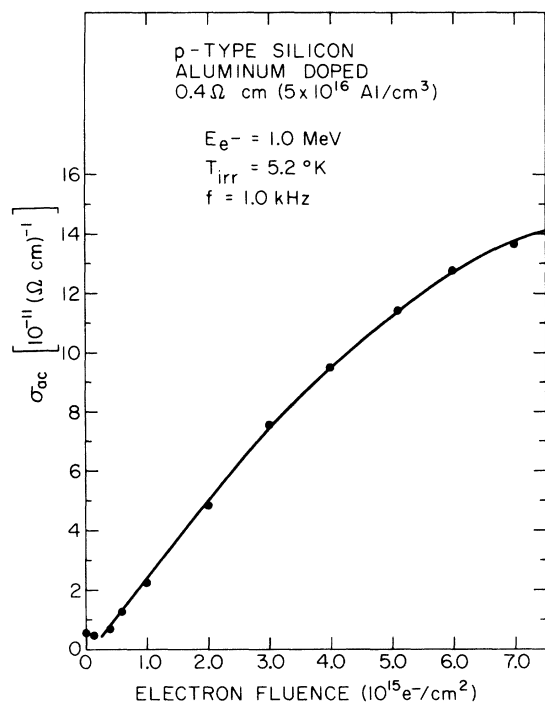
FIG. 4. Changes in σ_{ac} with irradiation for 0.4-Ω-cm
p-type silicon, aluminum doped.

upper limit on the surface conductance of 4.0×10^{-16}
Ω^{-1} per square of surface area. Samples typically
had only 5–10 squares of surface area between
front and back electrodes.

A. p-Type Silicon

The changes in σ_{ac} with electron fluence for p-
type aluminum-doped silicon for an irradiation
near 5 °K are shown in Figs. 3 and 4. The changes
are fairly linear with fluence, at least up to about
5.0×10^{15} e^{-}/cm^2, and illustrate that the measure-
ment of σ_{ac} can be used as a monitor of radiation
defects. The magnitude of the changes in σ_{ac} in-
crease as the aluminum concentration increases.
The changes in σ_{ac} with electron fluence for silicon
highly doped with boron $(1 \times 10^{17}$ B/cm$^3)$ are shown
in Fig. 5. Again note that the magnitude of σ_{ac}
after irradiation is large in a highly doped crystal.
After irradiation, samples typically showed a fre-
quency dependence of the form $\sigma_{ac} \sim \omega^s$, where s
ranged in value from 0.81 to 0.95 (see Fig. 6).
This compares with the value of $s = 0.79$ observed
by Pollak and Geballe[2] for crystals compensated
with chemical impurities. The frequency depen-
dence of the samples before irradiation did not
show any simple power-law dependence.

In n-type germanium, it is known[4] that the defects
responsible for the 65 °K annealing stage, following
irradiation by a 1.1-MeV electron beam, can be

annealed out by a 0.50-MeV electron beam in the
neighborhood of 5 °K. This "radiation annealing"
effect was also looked for in the silicon crystals
irradiated in this experiment. No radiation anneal-
ing effects were observed, due to either a 0.350-
or 0.500-MeV beam at temperatures of 1.5 or 4.5
°K. Typical results are shown in Fig. 7, and
suggest that the defects, perhaps the interstitials,
were mobile during the irradiation and formed
more complex defects (such as aluminum inter-
stitials) which do not radiation anneal.

We looked for differences in production rates in
p-type silicon between a 1.6 and a 5 °K irradiation.
If the onset of interstitial motion occurs in this
temperature region, one might expect a large tem-
perature dependence in the production rate. The
changes in σ_{ac} for a temperature of irradiation of
1.6 °K are shown in Figs. 8–10.

In Fig. 8, the changes in σ_{ac} during an irradiation
at 1.6 °K are compared to the changes observed
during a 4.8 °K irradiation. There is essentially
very little difference in the over-all production
rates. Figure 9 shows the changes observed in
σ_{ac} for a boron-doped crystal irradiated at 1.6 °K.
This crystal is doped to approximately the same
concentration of boron as the crystal of Fig. 8 was
doped with aluminum. The changes in σ_{ac} for a
given flux are essentially the same for these two
crystals. This indicates that the large changes in
σ_{ac} observed in a sample doped with 1.0×10^{17} B/
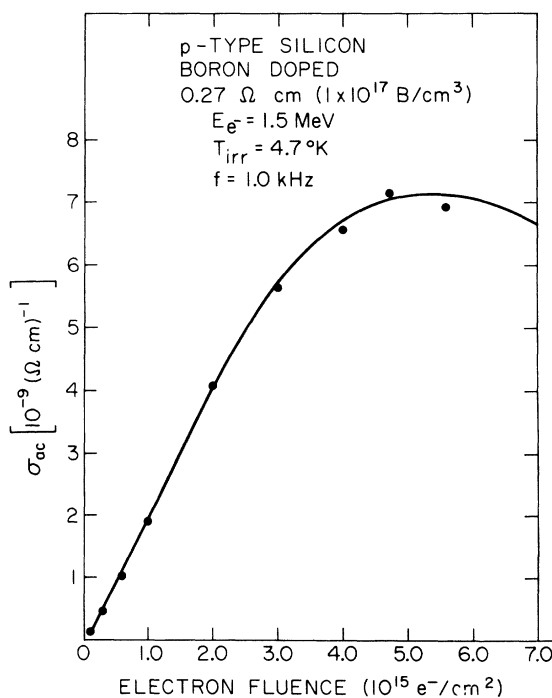
FIG. 5. Changes in σ_{ac} with irradiation for 0.27-Ω-
cm p-type silicon, boron doped.
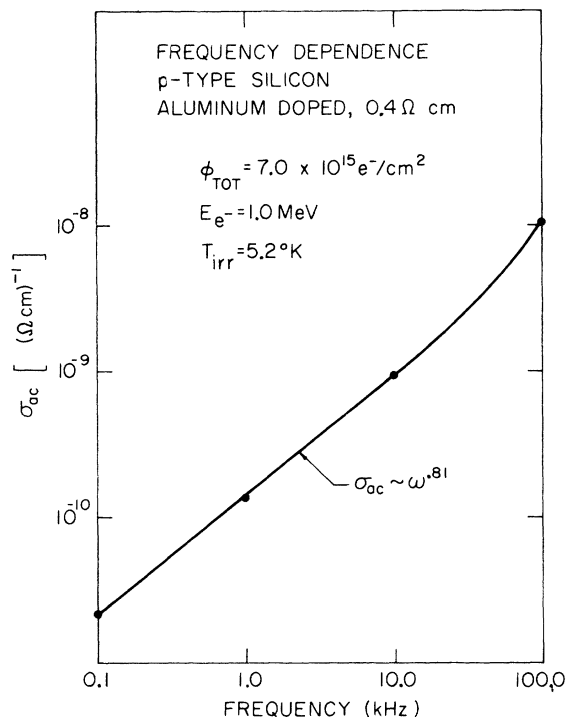
FIG. 6. Frequency dependence of σ_{ac} after irradiation of 0.4-Ω-cm p-type silicon, aluminum doped.

cm^2 are due to the concentration dependence and not due to the type of impurity. Figure 10 shows the changes in σ_{ac} for a crystal heavily doped with boron irradiated at 1.6 °K.

Under the supposition that the interstitial might suddenly become mobile, say somewhere between 1.3 and 4.2 °K, the samples were allowed to slowly warm from 1.3 to 4.2 °K at the end of the irradiation over a period of hours and measurements were

taken at various temperatures. Typical data are shown in Fig. 11. One expects σ_{ac} to increase with temperature because the tunneling rate is temperature dependent. The fact that σ_{ac} returned to its original value (triangular data point) upon cooling back down from 4.2 to 1.3 °K indicates that no irreversible changes, i.e., annealing of defects, took place in this temperature interval.

Isochronal anneals following irradiation were performed and typical results are shown in Fig. 12. No significant annealing stages were found below room temperature, indicating that the simple vacancies and interstitials formed by the electron collisions must have been transformed into defects that are stable at least up to room temperature. If the defects anneal, one would expect a decrease in σ_{ac}. However, a slight increase in σ_{ac} was usually observed upon warming to 20–30 °K. Further warming from 80 °K to room temperature usually brought σ_{ac} back to its post-irradiation value. It is felt that the slight increases in σ_{ac} are due to a small-charge trapping effect, similar to that observed by Calcott[5] in germanium.

B. n-type Silicon

The changes in σ_{ac} with electron fluence for n-type phorphorus-doped silicon due to a 1.0 -MeV beam are shown in Fig. 13 and for a 1.5-MeV beam in Fig. 14. The changes were proportional to electron energy and are linear with total electron fluence. After irradiation, n-type silicon showed a frequency dependence approximately of the form $\sigma_{ac} \simeq \omega^s$, with s ranging from 0.90 to 1.10. Previous measurements of the production rate of defects in n-type silicon at liquid-helium temperatures failed since the damage rate was too small to be measured in low to moderately doped crystals. However, changes in ac hopping conductivity are
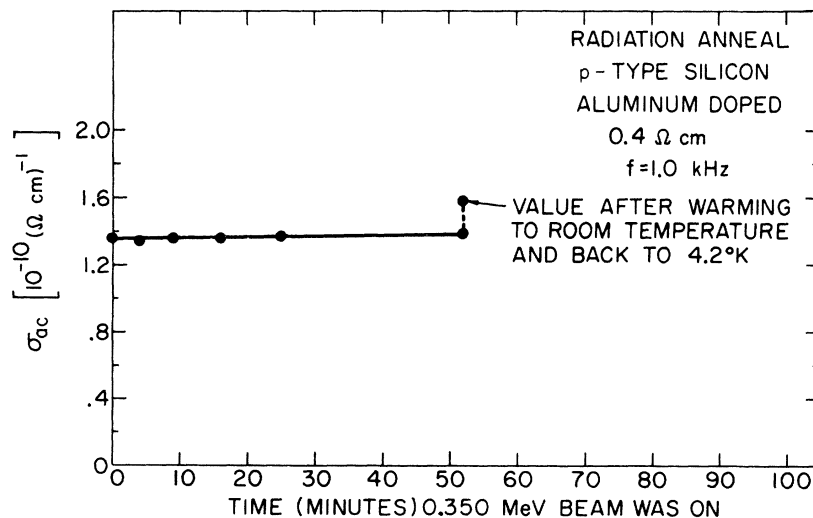
FIG. 7. Damage introduced by 1.0-MeV electron beam at 5.2 °K. Looked for radiation annealing effects at 5.8 °K using 0.350-MeV electron beam at 2.0×10^{-8} A/cm^2.
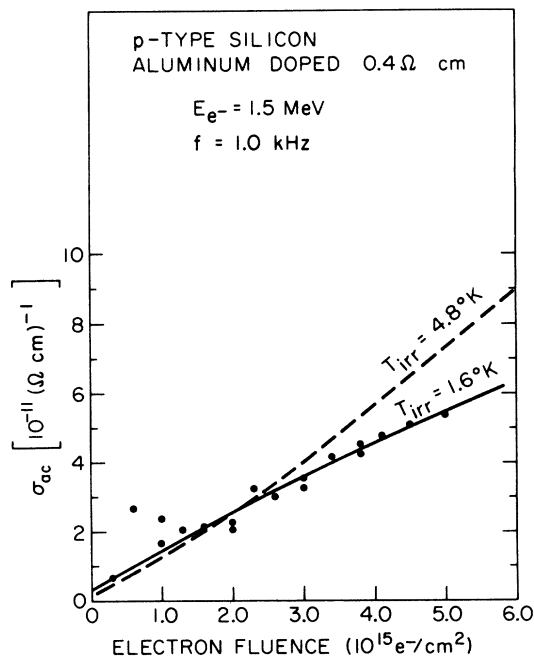
FIG. 8. Comparison of changes in σ_{ac} produced at irradiation temperatures of 4.8 and 1.6 °K in 0.4-Ω-cm p-type aluminum-doped silicon.
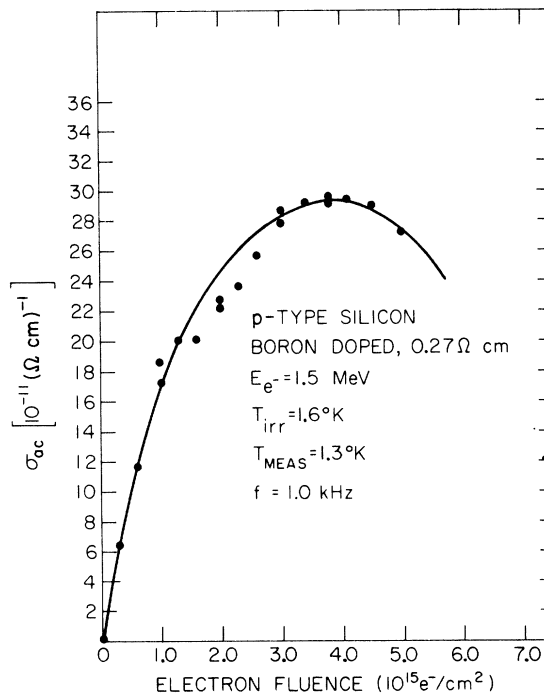
FIG. 10. Changes in σ_{ac} produced by irradiation at 1.6 °K of 0.27-Ω-cm boron-doped p-type silicon.
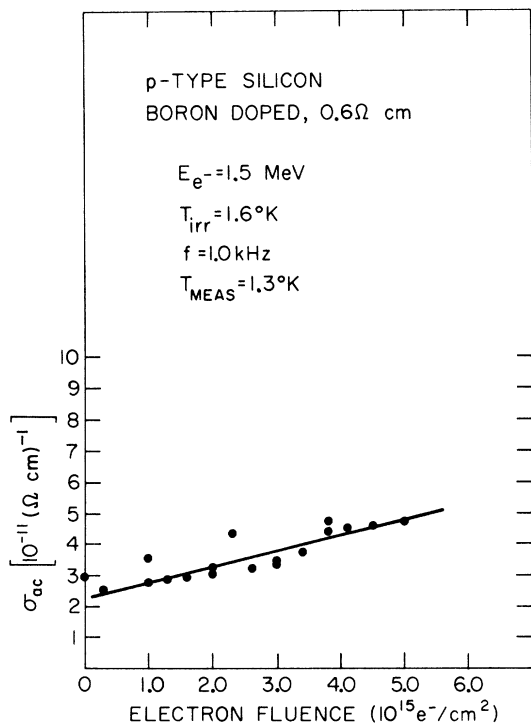
FIG. 9. Changes in σ_{ac} produced with irradiation at 1.6 °K of 0.6-Ω-cm boron-doped p-type silicon.

readily measured. n-type silicon was also irradiated at 1.6 °K to see if there was any significant difference compared to a 5.0 °K irradiation. This comparison is made in Fig. 15. The data taken at 1.6 °K showed considerable scatter. Also for the 5 °K runs, there was generally a variance in production rates of about ±20%. For these reasons it is not obvious that the differences in the two curves shown in Fig. 15 are significant.

At the end of the 1.6 °K irradiation, the sample was allowed to slowly warm up to 4.2 °K over a period of hours. Measurements were taken along the way at various temperatures, as shown in Fig. 16. The sample was then cooled back to 1.3 °K and the triangular data point was taken. The sample assumed a higher value of σ_{ac} after this procedure, whereas the p-type crystals came back to their original value.

Isochronal anneals were performed between 4.2 °K and room temperature and typical results are shown in Fig. 17. The samples were held at each anneal temperature shown for about 10 min and then returned to 4.2 °K for a reference measurement. No annealing stages were observed between 4.2 °K and room temperature although σ_{ac} typically increased on warming to 20–30 °K and there was usually a small decrease on warming to room temperature. These are probably charges trapping effects similar to those observed by Calcott in n-type germanium.
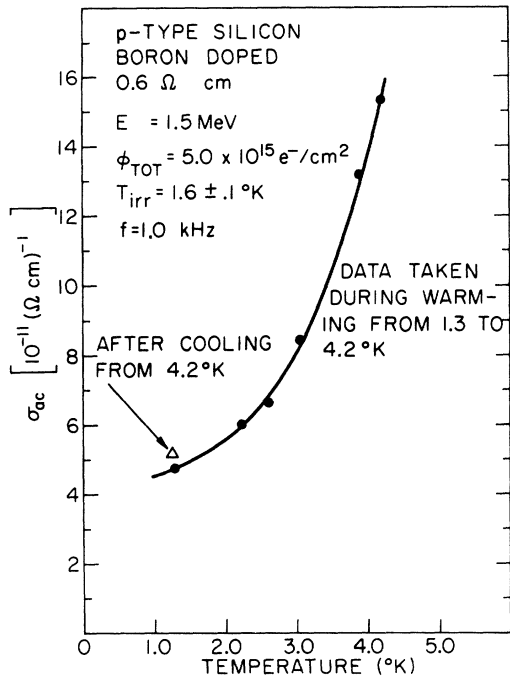
FIG. 11. Magnitude of σ_{ac} at various temperatures measured during warming from 1.3 °K to 4.2 °K and back to 1.3 °K at end of irradiation.

FIG. 13. Changes in σ_{ac} with irradiation for 0.54-Ω-cm n-type silicon doped with phosphorus.

an annealing process since an increase can also be observed upon warming to lower temperatures, say 20 °K.

Isothermal annealing was also done on one sample as shown in Fig. 18. The sample was held at 6.20 °K for roughly 15-min intervals and then measured at 4.2 °K. The hopping conductivity increased with the length of time held at 62 °K, but saturated after about 40 min. A plot of these data vs time$^{1/2}$ was not linear, and a logarithmic plot showed that they did not have a simple exponential dependence on time. Therefore, it is felt that these increases observed in σ_{ac} are not due to
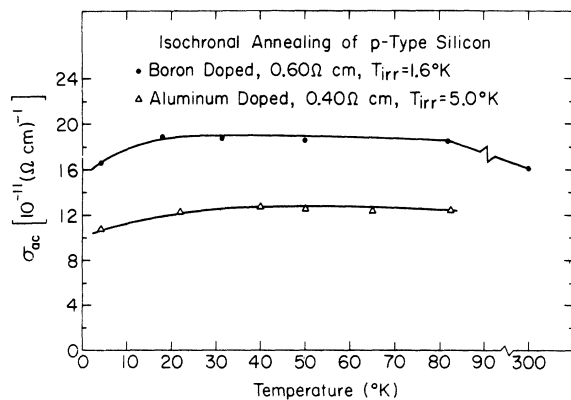
FIG. 12. Isochronal annealing of p-type silicon after irradiation. Measurements made at reference temperature of 4.2 °K and frequency of 1 kHz.

FIG. 14. Changes in σ_{ac} in 0.54-Ω-cm phosphorus-doped n-type silicon caused by irradiation with 1.5-MeV beam.
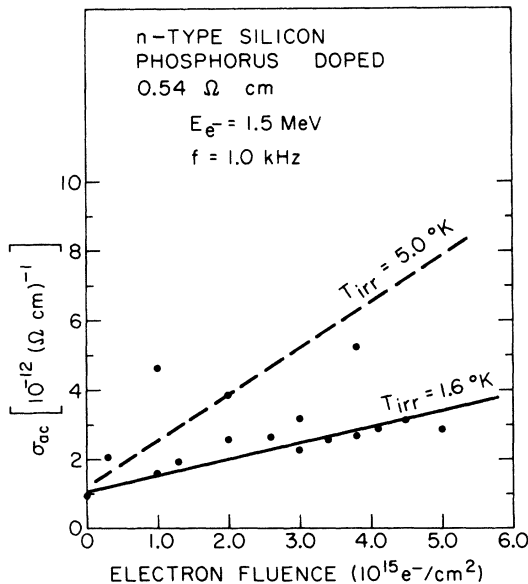
FIG. 15. Comparison of changes in σ_{ac} for 0.54-Ω-cm n-type phosphorus-doped silicon produced at irradiation temperatures of 5.0 and 1.6 °K, respectively.

The phenomenon of radiation annealing due to a low-energy beam was looked for in these n-type crystals with negative results. No radiation annealing effects were observed, as illustrated in Fig. 19, although there was a slight decrease in σ_{ac} after the first minute.

Not enough good data on n-type crystals of different doping levels were obtained to determine whether the production rate is concentration dependent.

C. High-Purity Silicon

High-purity crystals of silicon were irradiated and the changes due to a 1.0-MeV electron beam are shown in Fig. 20 and those due to a 2.0-MeV beam shown in Fig. 21. High-purity crystals typically have an impurity content of the order of 10^{13}/cm^3. Upon irradiation, these crystals would typically show a small initial increase in σ_{ac}, a saturation, and then perhaps a decline in σ_{ac}. It is felt that early in the irradiation the defects are compensating the small amount of impurities in the crystal but that the changes soon saturate as all the impurities become compensated and there are equal numbers of donor- and acceptor-type defects present. The fact that some changes can be measured in a high-purity sample indicates the sensitivity of the measurement of ac hopping conductivity.

A beam of 0.50-MeV electrons did not produce any radiation annealing effects in high-purity silicon.

Isochronal annealing of high-purity silicon fol-

lowing irradiation did not reveal any annealing "stages," but typically resulted in a gradual decrease in σ_{ac} as seen in Fig. 22.

V. DISCUSSION

The experimental data given above indicate a dependence of the damage production rate on the concentration of impurities in p-type silicon as monitored by ac hopping conductivity. If the model of Watkins is correct, one would expect the interstitials to be mobile during the irradiation. The interstitial would move around in the lattice until it came across a vacancy, which it would then annihilate, or if it encountered an impurity it might replace it. Therefore little net damage would result unless the interstitials were trapped along the way by impurities. This model predicts a dependence on impurity concentration in the defect production rate. The greater the number of impurities in the crystal, the greater the probability that the interstitials are trapped, preventing their recombination with vacancies.

Table II lists the average impurity separation for a range of dopant concentrations (using $N = \frac{1}{6}\pi d^3$, where d is the average impurity separation and N is the number of impurities per unit volume).

The nearest-neighbor distance in silicon is 2.35 Å; therefore it is readily seen that long-range motion of the interstitial is required if it is to be trapped by impurities.

We estimated the production rate of defects from the changes observed in σ_{ac}, assuming singly charged defects, and the results are summarized in Table III, for an electron energy of 1.50 MeV. The values are only rough estimates, good to $\pm 25\%$. The production rate is defined as the number of defects/cm^3 formed for each electron/cm^2 incident on the sample. The production rate in n-type silicon may be estimated from the magnitude of σ_{ac} by using the data of Pollak and Geballe[2,8] for a correspondence between σ_{ac} and the concentration of impurities (or defects). For the p-type crystals, the production rates were estimated by assuming that the maximum in the curve of σ_{ac} vs electron fluence for the highly boron-doped samples corresponded to a compensation ratio of about 0.5. The compen-

TABLE II. Impurity separation as a function of impurity concentration.

Impurity concentration N (cm^{-3})	Average impurity separation d (Å)
1.0×10^{13}	5759
1.0×10^{14}	2673
1.0×10^{15}	1241
1.0×10^{16}	576
1.0×10^{17}	267

n-TYPE SILICON
PHOSPHORUS DOPED
0.5 Ω cm

$E_{e^-} = 1.5$ MeV
$\phi_{TOT} = 5.0 \times 10^{15} e^-/cm^2$
$T_{irr} = 1.6 \pm .1 °K$
$f = 1.0$ kHz

AFTER COOLING
FROM 4.2

DATA TAKEN
DURING WARMING
FROM 1.3 TO 4.2°K

$\sigma_{ac} \left[10^{-12} (\Omega \, cm)^{-1} \right]$
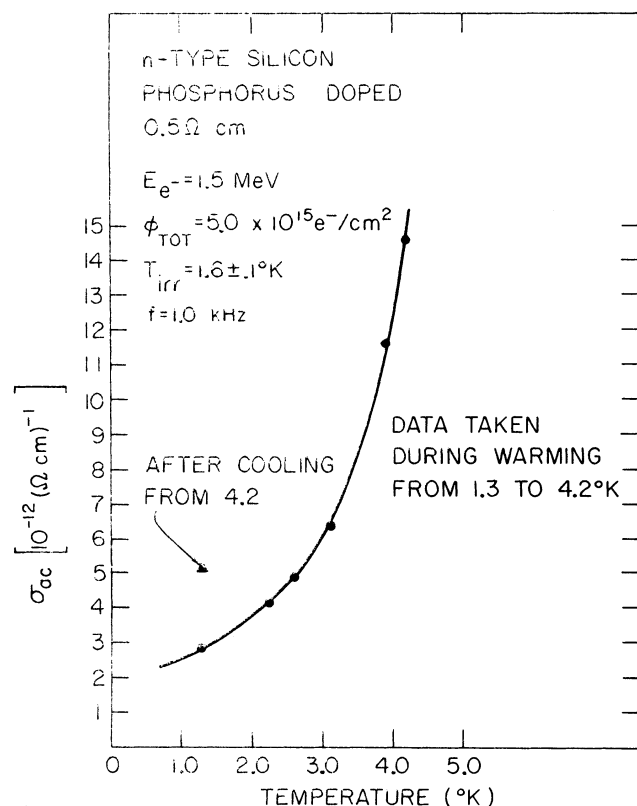
TEMPERATURE (°K)

FIG. 16. Magnitude of σ_{ac} as a function of temperature measured at various temperatures during warming from 1.3 to 4.2°K and back to 1.3°K after end of irradiation.

sation ratio is defined as the ratio of minority impurity (or defect) concentration to majority impurity concentration.

Table III shows that for p-type crystals, the defect production increases as the doping concentration increases. Note that for a crystal doped with 1.0×10^{17} B/cm^3, the production rate is 10.0 cm^{-1} assuming singly charged defects, or 5.0 cm^{-1} assuming doubly charged defects. The value of 5.0 cm^{-1} is very close to the theoretically calculated production rate for 1.5-MeV electrons. A displacement energy of 15 eV was used in this calculation.

It is useful to consider the possible charge states of the defects as a function of Fermi-energy level as depicted in Fig. 23. This scheme is based primarily on the work of Watkins for the vacancy

charge states. The charge states of the silicon interstitial are hypothetical and have not been experimentally determined, although Watkins feels that the interstitial has a positive charge state in a p-type lattice.

MacKay and Klontz[7] argue that during the irradiation the interstitials and vacancies will tend to be neutral in a radiation field since plenty of electrons and holes are being generated which can be trapped by charged defects, thus neutralizing them. However, there will be rapid oscillations of their charge states. The interstitial will be mostly neutral with frequent short periods of positive charge, and the vacancy will be mostly neutral with frequent short periods where it is either negative or positive, depending on the Fermi level.

TABLE III. Estimate of production rates of defects in irradiated crystals.

Crystal type	Dopant	Growth method	Resistivity (Ω cm)	Dopant concentration (cm^{-3})	Defect production rate (cm^{-1})
p	Aluminum	Float zone	4.0	3.3×10^{15}	0.03
p	Aluminum	Pulled	0.40	5.0×10^{16}	1.8
p	Boron	Float zone	0.60	3.0×10^{16}	1.8
p	Boron	Float zone	0.27	1.0×10^{17}	10.0
n	Phosphorus	Float zone	0.54	1.0×10^{16}	0.02
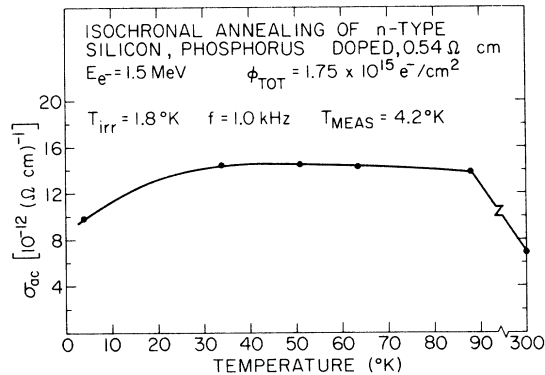
FIG. 17. Isochronal annealing of 0.54-Ω-cm n-type silicon after irradiation at 1.8 °K. Measurements made at reference temperature of 4.2 °K.

The MacKay-Klontz model says that during the irradiation the interstitials are neutral most of the time and move freely through the lattice. In p-type silicon, during the short periods when the defects are charged, the interstitial and vacancy probably both have a positive charge, resulting in a Coulomb repulsion between them, thus preventing annihilation. Furthermore, the positive interstitial will have a Coulomb attraction to the negative group-III impurities and if the interstitial can replace the impurity during this time, it is effectively trapped. Thus radiation damage is preserved in p-type silicon according to MacKay and Klontz.

In n-type silicon, the vacancy probably assumes a single or double negative charge when it is not in a neutral state during the irradiation. Thus there is no Coulomb repulsion with the interstitial in n-

type material. Moreover, during the short periods when the interstitial is positive, it will have a Coulomb repulsion with the positive group-V impurities. Therefore the most likely event is annihilation of the interstitial-vacancy pair. Thus n-type silicon has fewer defects remaining after irradiation than p-type silicon. A few of the interstitials and vacancies probably escape and give rise to the damage that is observed in n-type materials.

There have been at least two experiments since Watkins's which have used the model of long-range motion of the interstitial in their interpretation. One was that of Sivo and Klontz[8] and the other that of Cherki and Kalma.[9] In the experiment of Sivo and Klontz, n-type silicon irradiated at a relatively high temperature, say 120 °K, exhibited recovery when the irradiation was continued at a lower temperature, such as 30 °K. They argue that the meta-stable-pair model cannot explain this radiation annealing whereas a mobile interstitial model can. Cherki and Kalma studied the photoconductivity of defects in p-type silicon irradiation at 4.2, 20.4, and 77 °K. The p-type dopant was either aluminum or boron. They found that the position of the energy level arising from the defects was different for the two different dopants, aluminum or boron. They located the defect level by arbitrarily choosing the photon energy that excited 33% of the maximum number of carriers out of the defects. Following the results of Watkins, they concluded that the defects they observed must have been dopant interstitial atoms and that long-range motion of the silicon interstitial was involved.

Major questions yet remain to be answered. As yet no experiment has explicity shown that long-range motion of atoms has actually taken place. The charge states of the interstitial and the posi-
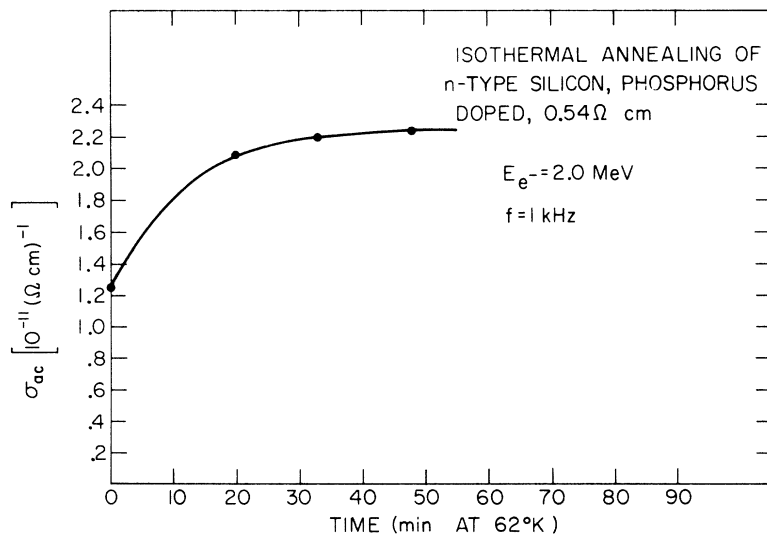
FIG. 18. Isothermal annealing of 0.54-Ω-cm n-type silicon after irradiation at 4.8 °K with 2.0-MeV electrons. Measurements made at reference temperature of 4.2 °K.
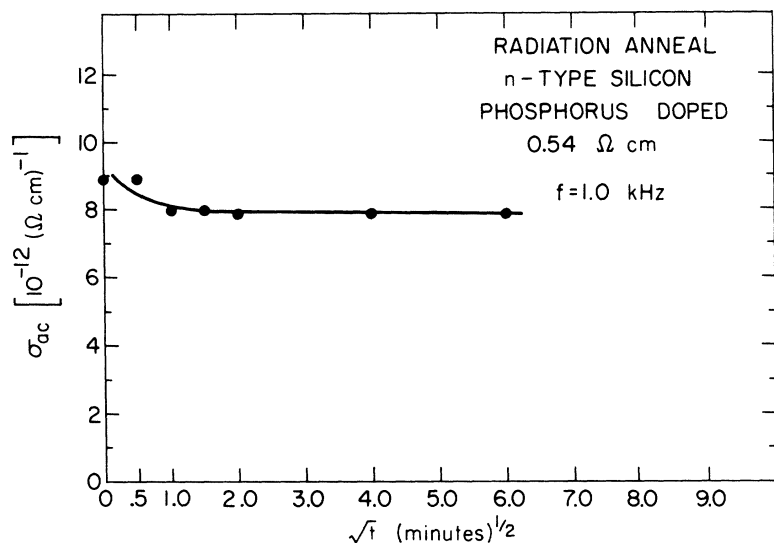
FIG. 19. Damage introduced by 2.00-MeV electron beam at 4.8 °K. Looked for radiation annealing effects at 5.0 °K using 0.500-MeV electron beam. t is the time in minutes that the 0.500-MeV beam was on.

tions of the corresponding energy levels in the band gap need to be determined. But to do this, the interstitials must be studied in their primordial state, before they have formed more complex defects. This may require working at temperatures below the value of 1.6 °K used in the present experiment. The geometrical configuration of the interstitial is unknown. There is also the mystery of why inter-

stitial silicon can move so readily at liquid-helium temperatures, whereas the group-III interstitials in silicon, at least interstitial aluminum and boron, do not migrate until a temperature of about 250–300 °C. If one examines all the diffusion data for silicon, then the interstitial impurities have the lowest known migration energies.[10] They are Li, 0.62 eV; Na, 0.72 eV; K, 0.75 eV; Cu, 0.43 eV; Au, 0.38 eV; note that these are about a hundred times larger than the thermal migration energy of
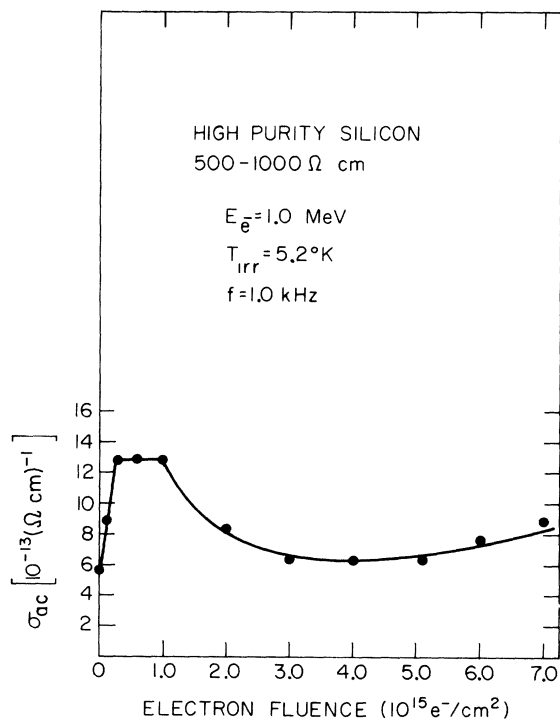
FIG. 20. Changes in σ_{ac} produced by irradiation of high-purity silicon at 5.2 °K with 1.0-MeV electrons.
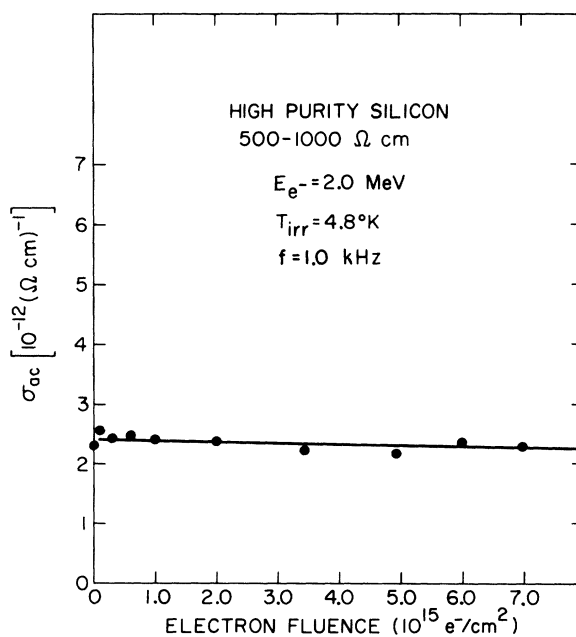
FIG. 21. Measurements of ac hopping conductivity in high-purity silicon irradiated at 4.8 °K with 2.0-MeV electrons.

ISOCHRONAL ANNEALING OF HIGH PURITY SILICON

500-1000 Ω cm

$E_{e^-} = 1.5$ MeV

$\phi_{TOT} = 7.5 \times 10^{15} e^-/cm^2$

$T_{irr} = 5.0\,°K$

$f = 1.0$ kHz
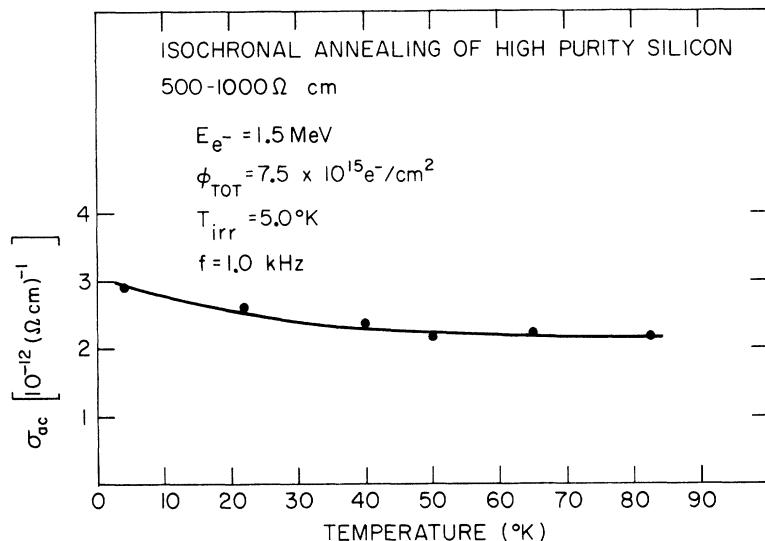
TEMPERATURE (°K)

FIG. 22. Isochronal annealing of high-purity silicon after irradiation at 5.0 °K with 1.50-MeV electrons. Measurements made at reference temperature of 4.2 °K.

a silicon interstitial would be if it migrates at 5 °K.

If the long-range migration of the interstitial silicon occurs by standard thermal-diffusion processes, one may estimate that its activation energy of migration is on the order of 0.002 eV. On the other hand, one must consider the possibility that athermal processes are responsible for the migration of the interstitial through the lattice during electron irradiation. It is conceivable that the silicon interstitial, once formed by primary knock on with the incident electron beam, is induced to make migration jumps through the lattice away from its parent vacancy by the following mechanisms: (i) energy transfer to the interstitial from collisions with the incident electron beam (the probability for this is small, however); (ii) energy transfer to the interstitial from collisions with secondary electrons produced by the primary electron beam; (iii) energy transfer from electron-hole recombination at recombination centers such as point defects (i.e., silicon interstitials); (iv) a 1.50-MeV electron traversing 150 μ of silicon loses about 52 keV in energy. An electron-hole pair is created for each 3.8 eV deposited in silicon, so that there are 1.37×10^4 pairs formed by each incident electron. As Shockley[11] points out, for each ionization event creating an electron-hole pair, there are 17.5 Raman phonons generated and each phonon has energy 0.063 eV in silicon. Therefore, for each electron in the primary beam, there are 2.4×10^5 phonons generated of energy 0.063 eV. For a beam current of 2.0×10^{-8} A/cm^2 as used in this experiment, this results in 3.0×10^{16} phonons/sec for each cm^2 of area. These phonons can coincide at the interstitial sites and cause diffusion jumps, resulting in long-range motion during the irradiation.

If the mechanisms mentioned above are the real

cause for easy motion of the interstitial, one would expect different results if the irradiation were done with a nonionizing particle such as thermal neutrons. If the long-range migration of the interstitial is related to the high ionization caused by electron irradiation, then the interstitial may not be mobile under conditions of neutron irradiation.

VI. SUMMARY AND CONCLUSIONS

The major results of this experimental investigation are: (a) σ_{ac} increased proportional to the electron fluence during the irradiation for both p- and n-type silicon; (b) although the production rate of defects in n-type silicon is small for a liquid-helium irradiation, changes in σ_{ac} could be readily monitored; (c) small initial changes could be detected in high-purity silicon but these saturated quickly; (d) the frequency dependence of σ_{ac} after irradiation was of the form $\sigma_{ac} \propto \omega^s$, where s ranged from 0.81 to 1.10, and is similar to that observed by Pollak and Geballe for chemically compensated
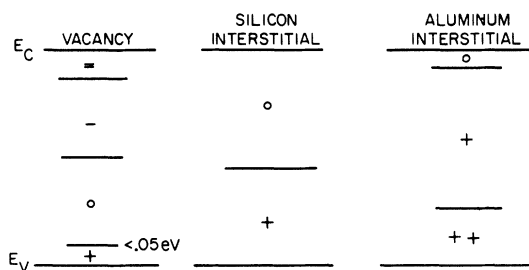
FIG. 23. Schematic diagram of the various charge states of different defects as a function of the position of the Fermi-energy level in the band gap of silicon.

samples; (e) there were no radiation annealing effects observed in p-type, n-type, or high-purity silicon at liquid-helium temperatures due to a low-energy (0. 35- or 0. 50-MeV) electron beam; (f) there was no significant thermal annealing below room temperature in p- or n-type silicon, although there was typically a small increase in σ_{ac} on warming to 20–30 °K; (g) the production rate of defects as determined by measurement of σ_{ac} was essentially the same at 1. 6 and 5. 0 °K (within a factor of 2) for both n- and p-type silicon; (h) the changes in σ_{ac} in p-type crystals were proportional to the concentration of p-type impurity, whether it be aluminum or boron; (i) an aluminum-doped crystal and a boron-doped crystal of similar concentration yielded similar changes in σ_{ac} with irradiation.

Results (e)–(h) together serve to confirm the suggestion of Watkins that the interstitial is mobile at liquid-helium temperatures and is either trapped at impurities or interchanges with them in a p-type lattice, creating impurity interstitials which migrate only above room temperature.

Measurement of ac hopping conductivity is cap-able of monitoring, for the first time, the small changes produced in nondegenerate n-type silicon during a liquid-helium-temperature irradiation. The data suggest that during the irradiation most of the interstitial-vacancy pairs recombine in n-type silicon, but a few remain at the end of the irradiation, accounting for the changes observed.

To our knowledge, this experiment is the first irradiation and measurement made on silicon below 4. 2 °K. We have irradiated silicon at 1. 6 ± 0. 1 °K and apparently have not prevented long-range motion of the interstitial in p-type silicon even at that temperature. The defects responsible for the 65 °K annealing stage in n-type germanium can be caused to radiation anneal at 5 °K with an apparent activation energy of 0. 0044 eV (presumably the interstitial).[12] Assuming that an Arrhenius-type relation for the diffusion constant is still valid in this temperature region, the interstitial in p-type silicon has an activation energy of migration of about 0. 002 eV. It is also possible that some athermal process associated with the large amount of ionization present produces the interstitial migration.

[1]G. D. Watkins, in *Radiation Damage in Semiconductors*, edited by P. Baruch (Dunod, Paris, 1965), p. 97.

[2]M. Pollak and T. H. Geballe, Phys. Rev. **122**, 1742 (1961).

[3]S. Gollin, Phys. Rev. **132**, 178 (1963).

[4]W. D. Hyatt, Ph. D. thesis (University of Illinois, 1970) (unpublished); J. W. MacKay and E. E. Klontz, J. Appl. Phys. **30**, 1269 (1959).

[5]T. A. Calcott and J. W. MacKay, Phys. Rev. **161**, 698 (1967).

[6]M. Pollak, Phys. Rev. **133**, A564 (1964).

[7]J. W. MacKay and E. E. Klontz, in *Radiation Effects in Semiconductors*, edited by F. L. Vook (Plenum, New York, 1968), p. 175.

[8]L. L. Sivo and E. E. Klontz, Phys. Rev. **178**, 1264 (1969).

[9]M. Cherki and A. H. Kalma, Phys. Rev. B **1**, 647 (1970).

[10]A. Seeger and K. P. Chik, Phys. Status Solidi **29**, 455 (1968).

[11]W. Shockley, Czech. J. Phys. **B11**, 81 (1961).

[12]W. D. Hyatt, Phys. Rev. (to be published).